Performance Analysis of a Spectral-Efficient High-Speed Hybrid PDM-MDM Enabled Integrated MMF-FSO Transmission

Somia A. Abd El-Mottaleb, Mehtab Singh, Hassan Yousif Ahmed, Median Zeghid, and Kottakkaran Sooppy Nisar

***Abstract*—This article proposes a novel 2 × 4 × 10 Gbps hybrid multi-mode-fiber (MMF) free-space optics-communication (FSOC) system based on integrating two multiplexing techniques; polarization-division-multiplexing (PDM) and mode-division-multiplexing (MDM). Two polarization states are used, each of these states carries four different Hermite Gaussian (HG) modes while each HG modes carries 10 Gbps data. Performance analysis is investigated by considering fixed length of MMF cable and varying FSOC range in absence and presence of different atmospheric turbulences (weak turbulence (WT) and strong turbulence (ST)). Additionally, it is evaluated also by taking a fixed range for FSO link and considering ideal scintillation with different MMF lengths. Moreover, it is investigated under rainy weather of Alexandria city in Egypt, Pune city in India, and Jeddah city in the Kingdom-of-Saudi-Arabia (KSA). The link distance, beam-angle, eye-diagrams, and bit-error-rate are the parameters that used for evaluating the system's performance. The results after simulating model using optisystem reveal 80 Gbps overall transmission capacity at 1500 m (100 m MMF + 1400 m FSO link) in the presence of ST, while for fixed FSO link (100 m), the achievable transmission is 350 m. The overall ranges of 1300 m, 1200 m, and 1600 m are achieved for Alexandria, Pune, and Jeddah.**

***Index Terms*—Polarization division multiplexing, multimode fiber, free space optics, Hermite Gaussian beams, bit error rate, beam divergence, atmospheric turbulences.**

Manuscript received 3 May 2023; revised 5 June 2023; accepted 26 June 2023. Date of publication 10 July 2023; date of current version 17 July 2023. This work was supported by Prince Sattam bin Abdulaziz University under Project PSAU/2023/R/1444. *(Corresponding author: Kottakkaran Sooppy Nisar.)*

Somia A. Abd El-Mottaleb is with the Department of Mechatronics Engineering, Alexandria Higher Institute of Engineering and Technology, Alexandria 21311, Egypt (e-mail: somaya8839@gmail.com).

Mehtab Singh is with the Department of Electronics and Communication Engineering, University Institute of Engineering, Chandigarh University, Mohali 140413, India (e-mail: mehtab91singh@gmail.com).

Hassan Yousif Ahmed is with the Department of Electrical Engineering, College of Engineering in Wadi Alddawasir, Prince Sattam Bin Abdulaziz University, Wadi Alddawasir 1191, Saudi Arabia (e-mail: hassanuofg@gmail.com).

Median Zeghid is with the Department of Electrical Engineering, College of Engineering in Wadi Alddawasir, Prince Sattam Bin Abdulaziz University, Wadi Alddawasir 1191, Saudi Arabia, and also with the Electronics and Micro-Electronics Laboratory (E. μ. E. L), Faculty of Sciences, University of Monastir, Monastir 5000, Tunisia (e-mail: m.zeghid@psau.edu.sa).

Kottakkaran Sooppy Nisar is with the Department of Mathematics, College of Science and Humanities in Alkharj, Prince Sattam Bin Abdulaziz University, Alkharj 11942, Saudi Arabia (e-mail: n.sooppy@psu.edu.sa).

Digital Object Identifier 10.1109/JPHOT.2023.3292550

I. Introduction

FREE space optical communication (FSOC) links are important in data transfer applications. It requires line of sight (LOS) transmission and uses atmosphere as a media in transferring the data [1]. Immunity to electromagnetic waves interference, low power consumption, high speed data transmission, implementation in urban areas, license-free spectrum, and large bandwidth are advantages of FSOC [2], [3]. These advantages make FSOC a good solution for solving problem of data traffic. However, the major factor that degrades the performance of the transmission link in the FSOC system is the atmospheric turbulence due to variations in temperature [5], [6]. Nowadays, the improvements in the optical fiber communication (OFC) technology have become remarkable. The exponential growth in internet technology and the variation in the types of applications like gaming systems have prompted increasing demand for transmission quality and data capacity [7]. Although there are several techniques used in OFC like wavelength division multiplexing (WDM) [8], [9], [10], time division multiplexing (TDM) [11], [12], and frequency division multiplexing (FDM) [13], the data transmission rates and spectral efficiency are not satisfactory. The existing technologies of optical data transmission using OFC like single mode fibers (SMFs) will reach their capacity limits [14], [15], and that according to Shannon's limit [16]. So, the requirement of using multimode fiber (MMF) cables has increased as they provide high bandwidth.

Thus, using MMF with FSOC will result in enhancement in transmission capacity and will be reachable everywhere. Furthermore, for more capacity enhancement, different multiplexing techniques are used in FSOC systems like polarization division multiplexing (PDM) [17], orthogonal FDM [18], and mode division multiplexing (MDM) [1], [19].

PDM is a multiplexing technique where one or more polarization signals are combined leading to generation of new parallel state. The transmission data capacity is enhanced in PDM through allowing distinct signals transmitting their data in an orthogonal beam using same wavelength [20], [21].

MDM is a recent technique that is used in optical communication networks either MMF or FSOC due to its ability for providing high data transportation [22]. It uses eigen modes for transmitting independent channels at the same time. Modes like Laguerre-Gaussian [23], orbital angular momentum [1],

[24], and Hermite-Gaussian [25] are used MDM techniques for capacity enhancement.

The Hermite-Gaussian (HG) beams are the solutions to the paraxial wave equation (Cartesian coordinate system) that form set of functions with Gaussian beam which are orthogonal and complete and known as modes of propagations [26].

Recently, there are several studies using either MDM or PDM in FSOC transmission only, OFC transmission only, and both hybrid OFC with FSOC transmission. In [27], PDM is used with FSOC transmission system. Ten channels coded by random diagonal code of spectral amplitude coding optical code division multiple access (SACOCDMA) are transmitted on two polarization states and a transmission capacity of 50 Gbps is achieved. In [28], six channels assigned by diagonal permutation shift code of SACOCDMA system are used in hybrid PDM/FSOC system. The conducted results reveal a capacity enhancement of 60 Gbps. In [1] MDM is used with FSOC transmission system. Two distinct Laguerre-Gaussian (LG) beams are used; each carrying three different channels encoded by fixed right shift code of SACOCDMA system. An overall transmission capacity of 60 Gbps is achieved. Four different LG beams are used in MDM/FSOC transmission in [24] and a 40 Gbps transmission data capacity is achieved. In [29], two different modes are used in MDM/ FSOC transmission communication system and a successful transmission of 10 Gbps is reported.

In [30], MDM is used in hybrid MMF/FSOC transmission. Two distinct modes and a transmission capacity of 80 Gbps after 100 m MMF length and 2070 m FSOC range is achieved. In [31], MDM in OFC system using code division multiplexing is proposed. The linearly polarized (LP) modes are used and the results show that the system can transmit up to 42 km distance with a transmission capacity of 80 Gbps. In [32], the LP modes are used in MDM-passive optical network system with OCDMA system. Two fibers are used, SMF and two mode fiber (TMF). The obtained results reveal that the system achieves a transmission capacity of 80 Gbps with 40 km SMF length and 2 km TMF length.

In this article, for the first time according to our knowledge, we will use PDM with four HG modes in hybrid MMF/FSOC system for enhancing transmission capacity. The main contributions are:

- Introducing a new high speed transmission of MMF-FSOC system based on combining PDM with MDM using four HG modes (HG00, HG01, HG10, and HG11).
- Investigate the effect of beam divergence and atmospheric turbulence, which are major factors that cause degradation to the FSOC link.
- Evaluate the performance of the suggested model based on actual metrological data from three cities located in different countries; Alexandria in Egypt, Pune in India, and Jeddah in KSA.

In this article, a new hybrid MMF/FSOC system based on combining PDM with MDM is proposed for capacity enhancement. Two polarization states are used. The first one is used for transmitting the optical signals that carries the information data on X-polarization (X-PL) state. These signals are transmitted using four different HG beams (HG00, HG01, HG10, and HG11), which each beam transports 10 Gbps. The second polarization state is used for transmitting the information signal on Y-polarization (Y-PL) state. Also, this state is used for transmitting the data that uses four different HG beams. Thus, a capacity enhancement is achieved as the total transmission data is 2 PDM $\times$ 4 HG modes $\times$ 10 Gbps $=$ 80 Gbps. The performance is investigated considering two cases, the first case is using fixed MMF cable length of 100 m and varying FSOC range. In this case, the effect of different beam divergence and the turbulences effects like weak turbulence (WT) and strong turbulence (ST) on the performance of the proposed model is investigated. As for the other case, a fixed FSOC of 100 m is used while the length of MMF is varied. Further, the performance is evaluated using real meteorological data from different cities in different countries.

The organization of the rest of the article is as follows. Sections II and III give a brief explanation of HG modes and MMF cable. A description of the proposed PDM/MDM based MMF/FSOC transmission is given in Section IV, followed by the performance analysis in Section V. Sections VI and VII show the simulation results with discussion and the main conclusion, respectively.

II. HG Modes

Lasers are used in different areas of optics. The transverse mode (TM) is the field distribution that is orthogonal to the direction of the laser's propagation, and when there are different spatial modes, there will be different TMs that correspond to them [33]. The HG modes are a full collection of spatial modes with orthogonal bases, and any spatially distributed pattern can be extended using the HG mode basis [34]. They are higher order modes of Gaussian beam which are generated by using the solutions of the higher-order of the paraxial equation with Hermite polynomials in rectangular coordinates [35], [36], [37], [38]. The $HGmn$ modes are distinguished by two indices, m indicating the number of nodes in the horizontal axis and n indicating the number of nodes in the vertical axis. In Cartesian coordinate system, the electric field of the HG beam, $E_{HGmn}(x,\ y,\ z)$, is expressed as [39].

$$E_{HGmn}(x,y,z) = \sqrt{\frac{2}{\pi n!m!}}2^{-\left(\frac{n+m}{2}\right)}exp \times \left[-i\left(\frac{k\left(x^2+y^2\right)}{2R\left(z\right)}\right)\right]\exp\left[-i\left(n+m+1\right)\right] H_m\left(\frac{\sqrt{2y}}{w}\right)H_n\left(\frac{\sqrt{2x}}{w}\right)\exp\left(\frac{-(x^2+y^2)}{w^2}\right) \quad (1)$$

where H_m (.) and H_n(.) are Hermite polynomials of order m in x direction and n in y direction, respectively, k is a wave number and equal to $(2\pi/\lambda)$ where λ is the optical wavelength, $R(z)$ is the beam curvature, and w indicates the beam spot size. The HG beams are used in FSOC systems applications due to its ability to enhance the capacity using MDM [40]. In this article, the vertical-cavity surface-emitting laser (VCSEL) component is used from optisystem software version 19 for generating

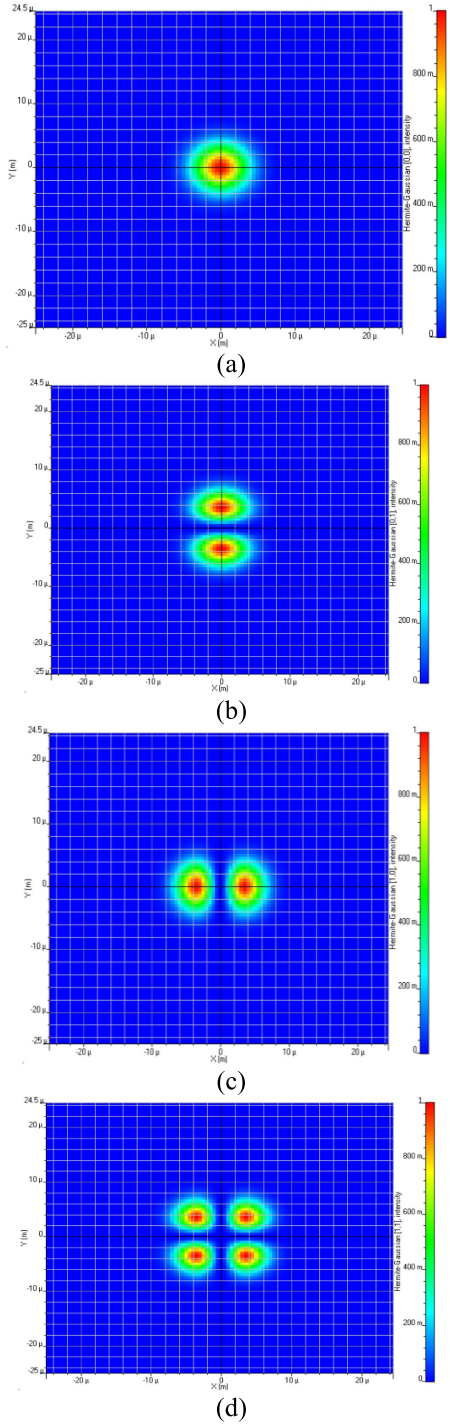

Fig. 1. Intensity profiles for different HG modes: (a) HG00, (b) HG01, (c) HG10, and (d) HG11.

different HG modes. The HG modes that considered in this study are HG00, HG01, HG10, and HG11 and their intensity is given in Fig. 1.

For more capacity enhancement, PDM is used with HG modes. Fig. 2 illustrates how PDM combines with MDM using the HG 01 beam. Using the same HG01 beam, two information data are sent on a single wavelength (λ_1). The first data is sent on the X-PL signal, while the second data is sent on the Y-PL signal.

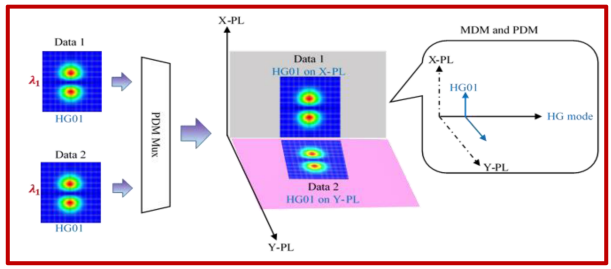

Fig. 2. Concept of combining PDM with MDM using HG01 beam.

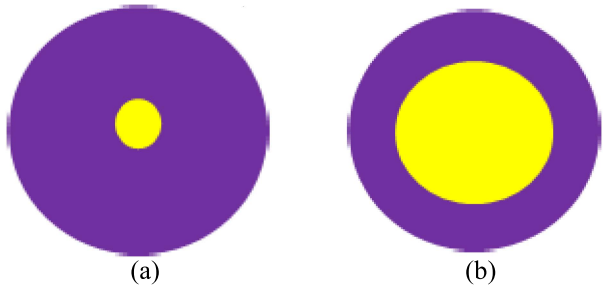

Fig. 3. Different types of OFC cables. (a) SMF and (b) MMF.

Then both signals are multiplexed using a PDM multiplexer and sent together at the same time.

III. MMF Channel

Recently, the development of OFC has enabled the development of different types of optical fibers like SMF and MMF as shown in Fig. 3. Optical fiber is classified into two types according to the number of modes. The SMF has small core diameter (8-10 μm) so it allows only one mode to propagate in its core. On the contrary, the MMF has large core diameters (50-100 μm), so multiple modes can propagate along the fiber leading to capacity enhancement [41].

Accordingly, in this work, the MMF cable is used in which its refractive index, $n(r)$ is expressed as [42]

$$n\left(r\right) = n_{\infty}(1 - \Delta r^{\alpha_P} \tag{2}$$

where n_{∞}, Δ, r, and α_P, are maximum refractive index of the core, profile height parameter, normalized radial distance from the center of the core, and profile alpha parameter of the $n(r)$, respectively. At the input of the MMF, the total incident spatial electric field, $E^i_{qd}(r, \theta,\ t)$ is given as [42]

$$E^i_{qd}\left(r,\theta,t\right) = \left[\sum_q \sum_d c_{qd} e_{dq}\left(t\right)\right] E^i_{qd}\left(r,\theta\right) \tag{3}$$

where q and d are azimuthal mode number and radial mode number, respectively, c_{qd} is the power coupling coefficient, and e_{dq} is the transverse electric field of the HG modes.

As for the output electric field, it is expressed as [42]

$$E_o\left(r,\theta,t\right) = c_{qd} e_{dq}\left(t - \tau_w\right) E^i_{qd}\left(r,\theta\right) e^{j\beta_w z} \tag{4}$$

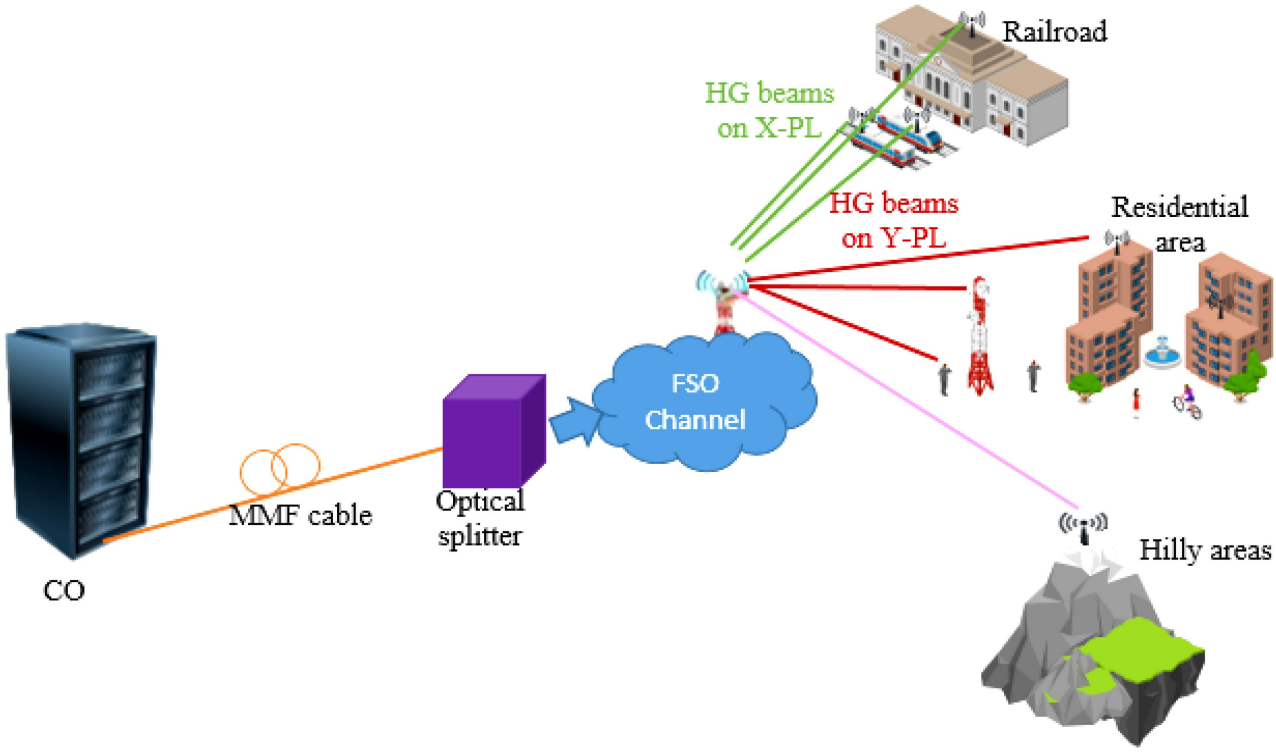

Fig. 4. Layout of PDM/MDM based MMF/FSOC system.

where τ_w is the time delay and β_w is the propagation constant of the degenerate mode group w. The attenuation, γ_{MMF}, is expressed as [43]

$$\gamma_{MMF} = \gamma_{MMFo}\left\{1 + I_p \times\left[\eta\left(\left(\lambda(|q|+2d)/(2\pi r n_{co})\left[(\alpha_P+2)/(\alpha_P\Delta)\right]^{0.5}\right)^{\frac{2\alpha_P}{\alpha_P+2}}\right]\right\} \tag{5}$$

where γ_{MMFo}, I_p, and η, are basic attenuation by all modes, p-th order modified Bessel function of the first kind, and scaling factor.

IV. Proposed PDM/MDM Based MMF/FSOC Transmission

Fig. 4 shows the schematic diagram that shows the layout of the MMF-FSOC system based on combining PDM with 4 HG modes. It consists of the central office (CO), MMF, FSO, optical wireless unit, and users. The CO contains the information data that is required to be transmitted to the user's premises. The data is first modulated onto optical wavelengths and then combined before being delivered to the propagation channels. Here, two channels are assumed, which are MMF cable and FSOC link, to be able to reach areas where implementation of OFC is difficult, like mountains. Further, an optical splitter is used to split the data, and then the data reaches its destination.

As any communication system consists of three main parts: the transmitter, channel, and receiver, our proposed PDM/MDM based MMF/FSOC transmission has the same three parts as shown in Fig. 5. At the transmitter, a VCSEL source centered at 1550 nm is used to generate four HG modes (HG00, HG01, HG10, and HG11) first on X-PL by setting the azimuth angle at 0^{o} and second on Y-PL by setting the azimuth angle at 90^{o}. Each HG mode carries 10 Gbps data. This data is generated from a pseudo-random bit sequence generator (PRBSG) and then entered into a non-return-to-zero (NRZ) on-off keying electrical modulator. To be able to transmit this data through optical HG modes, it must first be converted to an optical signal by using a Mach-Zehnder modulator (MZM). The overall 40 Gbps that are transmitted on four different HGs using either X-PL or Y-PL are multiplexed by using an MDM multiplexer. A PDM combiner (PC) is then used to combine both the data signals that were transmitted on X-PL and Y-PL before transferring them to the propagation channel. Here, two channels are used with two cases. In the first case, a 100 m fixed length of MMF cable is used with varying propagation ranges, while in the second case, increasing lengths for MMF cable are considered with a fixed FSO propagation range of 100 m. At the receiver, the received signal is first split by a PDM splitter (PS) into an X-PL signal and a Y-PL signal. The received signal in either X-PL or Y-PL is further separated into four HG modes through the use of an MDM demultiplexer. A photodetector (PD) is used to detect the required information signal corresponding to the HG mode and to convert the optical signal to an electrical signal. A low pass filter (LPF) is then used for filtering the signal, and for

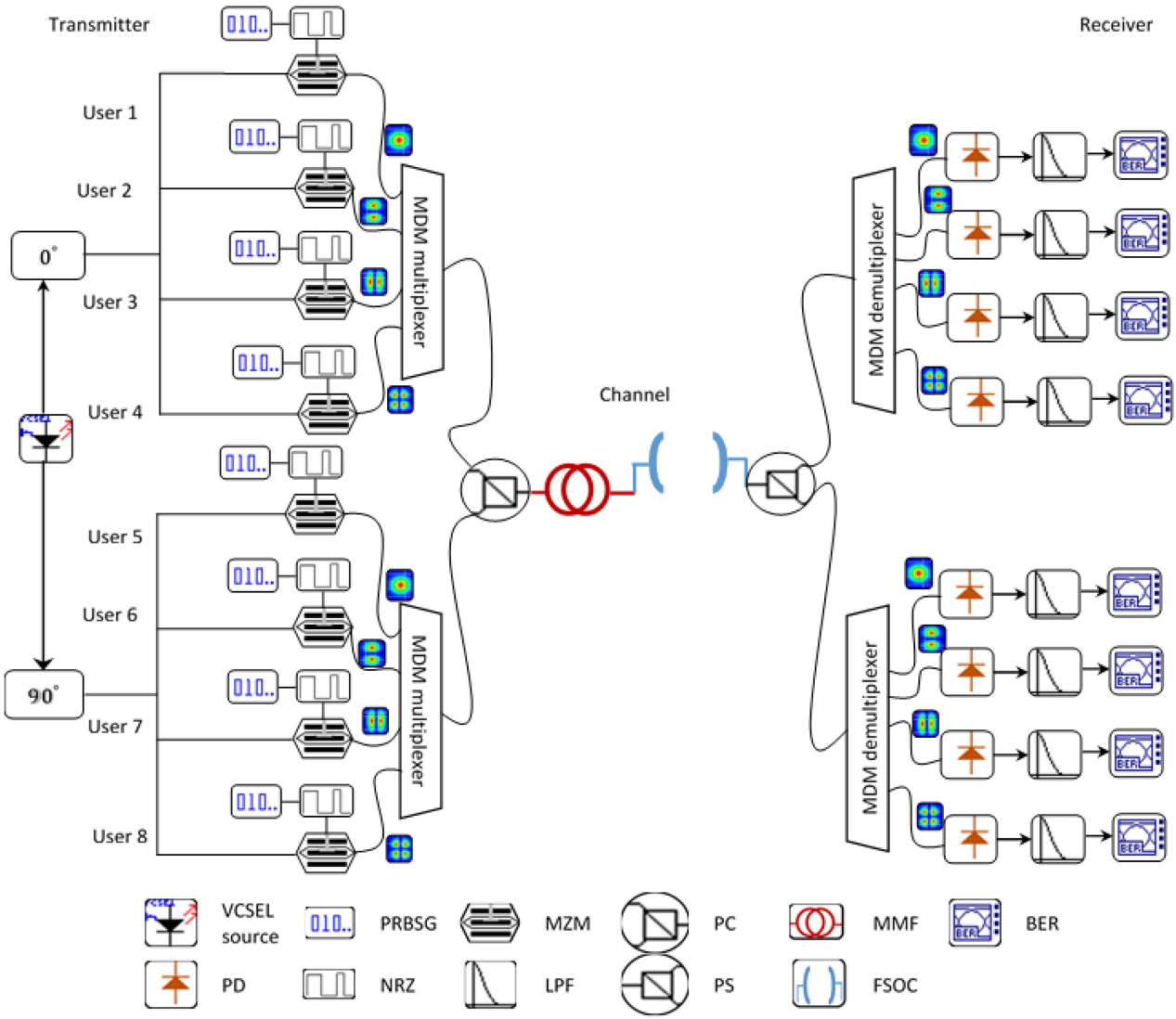

Fig. 5. Schematic diagram of PDM/MDM based MMF/FSOC transmission.

analyzing the performance of the received information signal, a BER analyzer is used.

V. Performance Analysis of PDM/MDM Based MMF/FSOC Transmission

The received current at the PD is [44]

$$I = S_R B_{op} \Re \tag{6}$$

where B_{op} and $\Re$ are the optical bandwidth and the responsivity of the PD, respectively. Parameter S_R indicates the received power and is expressed as [17]

$$S_R = S_T \left(\frac{d_R}{d_T + \Phi L} \right)^2 10^{\frac{-\beta L}{10}} \tag{7}$$

where S_T is the transmitted power, d_T and d_R are transmitter and receiver aperture diameter, respectively, Φ indicates the beam divergence angle, L is the FSO range, and β is the atmospheric attenuation. As there is variation in temperature during the propagation of the information signal in the FSOC channel, so this leads to atmospheric turbulence which varies from weak turbulence (WT) to strong turbulence (ST). Models like gamma-gamma, log-normal, and K-distribution are used for modelling the channel under the effect of atmospheric turbulence [6], [45]. Under the effect of WT and CA weather conditions, log-normal model is used [6], while for ST, K-distribution model is used [45]. As for gamma-gamma distribution, it is commonly used as it can be used for both WT and ST [46]. Accordingly, gamma –gamma model is considered in this study. In gamma-gamma, the normalized intensity of light is defined by α and γ, which are large and small edges scales, respectively. The probability density function is given as [47], [48]

$$PDF\left(I_s\right) = \frac{2(\propto \gamma)^{\frac{\alpha+\gamma}{2}}}{\Gamma(\alpha)\Gamma(\gamma)} I_s^{\frac{(\alpha+\gamma)}{2}} K_{\alpha-\gamma}\left(2\sqrt{\alpha\gamma h_s}\right); h_s > 0 \tag{8}$$

$$\alpha = \left[\frac{0.51\sigma_r^2}{\left(1 + 0.69\sigma_r^{12/5}\right)^{5/6}} \right] - 1 \quad (9)$$

$$\gamma = \left[\frac{0.49\sigma_r^2}{\left(1 + 1.11\sigma_r^{12/5}\right)^{5/6}} \right] - 1 \quad (10)$$

where $K_j(.)$, and $\Gamma(.)$ are the j^{th}order of modified Bessel function and the Gamma function, respectively, and $\sigma_r^2$is the Rytov variance which differs according to the value of the refractive index,C_n^2 and is expressed as [49]

$$\sigma_R^2 = 1.23 C_n^2 K^{7/6} R_{FSO}^{11/6} \quad (11)$$

where K is the wave number and equal to $(2\pi/\lambda)$. The values of C_n^2 for WT, MT, and ST, are 1×10^{-17} $\mathrm{m}^{-2/3}$, 5×10^{-15} $\mathrm{m}^{-2/3}$, and 1×10^{-13} $\mathrm{m}^{-2/3}$, respectively. Moreover, the different FSO propagation ranges can be distinguished by the σ_R^2, as if $\sigma_R^2 < 1$, then that means WT occurs, while if $\sigma_R^2 \sim 1$, then MT occurs, and if $\sigma_R^2 > 1$, so there is ST and if σ_R^2 goes to infinity then that means that turbulence is saturated.

The signal to noise ratio (SNR) is expressed as [17], [28]:

$$SNR = \frac{(I)^2}{\sigma_{Sh}^2 + \sigma_{th}^2} \quad (12)$$

where $\sigma_{Sh}^2$is the shot noise and equals to 2e $\upsilon\Re < I >$, (e is the charge of the electron and υ is the electrical bandwidth), and σ_{th}^2 refers to the thermal noise and expressed as [28]

$$\sigma_{th}^2 = {4k_B T\upsilon}/{r_L} \quad (13)$$

where k_B and T, are respectively, Boltzmann constant and absolute temperature of receiver, and r_L is the load resistance.

Finally, the BER is given as [28]

$$\mathrm{BER} = \frac{1}{2} erfc\left(\frac{\sqrt{\mathrm{SNR}}}{2\sqrt{2}}\right) \quad (14)$$

where erfc refers to the error complementary function.

VI. Results and Discussion

The proposed PDM/MDM based MMF/FSOC transmission system using 4 HG modes is simulated using Optisystem Software ver. 19 with the parameters given in Table I [4], [17], [27], [30]. The performance of the proposed model is evaluated in terms of beam divergence, MMF length, FSO propagation range, eye diagrams and log(BER). The simulation results are divided into four parts. The effect of difference beam divergence on system performance, is discussed in the first part. In the second part, the performance is investigated for the proposed PDM/MDM based MMF/FSOC transmission at a fixed length of 100 m of the MMF cable while varying the FSO range under clear air (CA) weather conditions. The third part shows impact of atmospheric turbulences on the performance of the received information signal, followed by the effect of different MMF lengths on the performance of the proposed model at a constant FSO range of 100 m in the fourth part. Finally, the fifth part shows the performance of the proposed model under the rainy weather for Alexandria city in Egypt, Pune city in India, and Jeddah city in KSA.

TABLE I
Proposed Model Parameters [4], [17], [27], [30]

Parameter	value
Input power of the VCSEL source	15 dBm
HG modes	HG00, HG01, HG10, and HG11
Centered wavelength	1550 nm
Polarization states	X-PL at 0° azimuthal angle Y-PL at 90° azimuthal angle
Data rate per channel	10 Gbps
Electrical bandwidth	0.75×Bit rate Hz
Linewidth of VCSEL	10 MHz
MMF Length	100 m
MMF cable attenuation	2.61 dB/km
Angle of beam divergence	2 mrad
Transmitter aperture diameter	10 cm
CA weather attenuation	0.14 dB/km
Atmospheric turbulences considered	WT and ST
Turbulence model	Gamma-Gamma distribution
Receiver aperture diameter	20 cm
Responsivity of the PD	1 A/W
Noise temperature and load resistance of the receiver, respectively	300 K and 1030 Ω, respectively.
Thermal noise power density	10^{-22}W/Hz

A. Effect of Beam Divergence on the Performance of the Proposed System

Beam divergence has an effect on the information signal during transmission in the FSO channel. Ideal scintillation (no atmospheric turbulence), a fixed MMF length of 100 m, and a fixed FSO range of 800 m are considered. Fig. 6 shows the log (BER) performance of the proposed PDM/MDM based MMF/FSOC system versus different angles of beam divergence. The performance of users 1–4 that transmitted on X-PL using four different HG modes is shown in Fig. 6(a), while the performance of users 5–8 that transmitted on Y-PL using the same HG modes is displayed in Fig. 6(b). It is clear that as the divergence angle increased, the performance is degraded for all users. As an

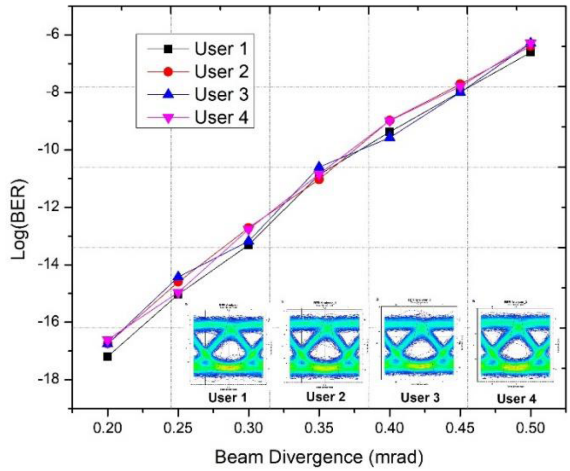

(a)

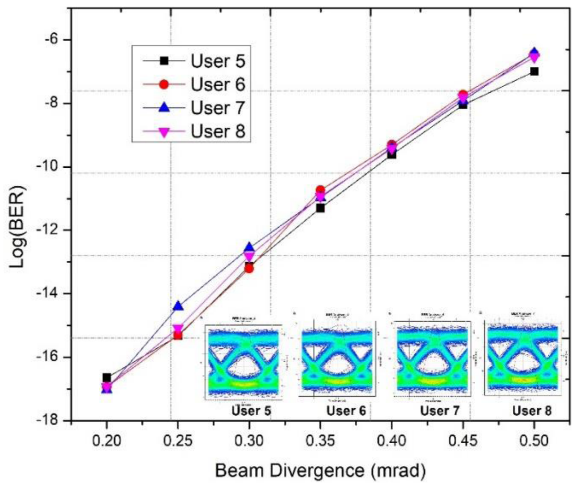

(b)

Fig. 6. Log(BER) for proposed PDM/MDM based MMF/FSOC transmission versus beam divergence angle for (a) users 1–4 transmitted on X-PL and (b) users 5–8 transmitted on Y-PL.

example, at a beam divergence angle of 0.2 mrad., the log(BER) of user 1 is −17.19, which is increased to −6.6 when the beam divergence angle is increased to 0.5 mrad. Also, the large eye openings for the all users that are transmitted using four HG modes on two different polarization states at a beam divergence angle of 0.5 mrad. indicate reliable received data.

Table II tabulates the log(BER) values for the all users at a beam divergence angle of 0.5 mrad.

B. Effect of Different FSO Propagation Range on the Performance of the Proposed System

In this part, the fixed MMF of 100 m, CA weather conditions, ideal scintillation, and various FSO ranges from 800 m to 1400 m are considered. The measured log(BER) for users 1, 2, 3, and 4 that transmitted using HG00, HG01, HG10, and HG11 modes, respectively on X-PL signal for proposed model versus FSO ranges is given in Fig. 7(a) while Fig. 7(b) depicts the log(BER)

TABLE II
LOG(BER) VALUES FOR ALL USERS CORRESPONDING TO 0.5 MRAD DIVERGENCE ANGLE

Users	HG modes	Polarization state	Log(BER)
1	HG00	X-PL	-6.60
2	HG01		-6.39
3	HG10		-6.29
4	HG11		-6.27
5	HG00	Y-PL	-6.99
6	HG01		-6.43
7	HG10		-6.41
8	HG 11		-6.54

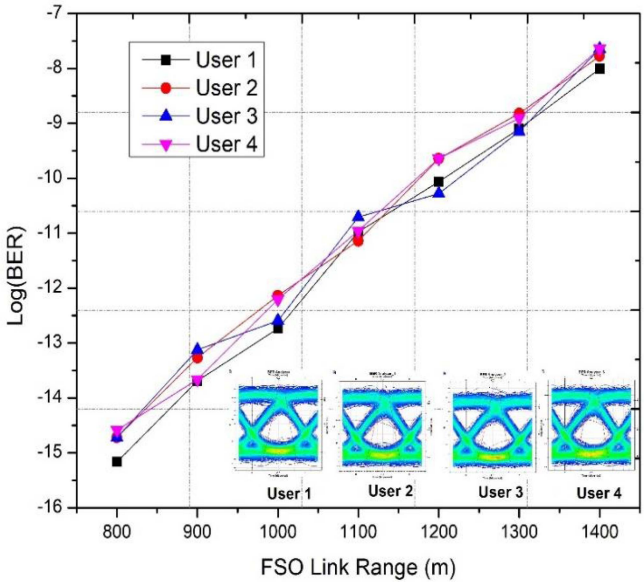

(a)

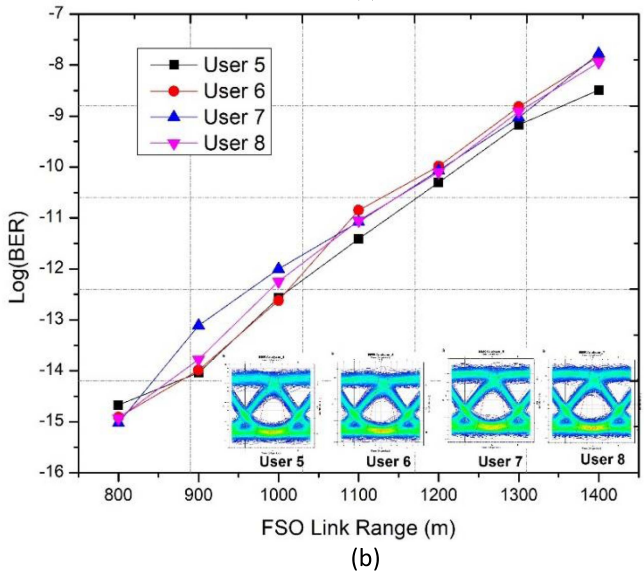

(b)

Fig. 7. Log(BER) for proposed PDM/MDM based MMF/FSOC transmission after a fixed MMF of 100 m versus different FSO links under CA for (a) users 1–4 transmitted on X-PL and (b) users 5–8 transmitted on Y-PL.

TABLE III
LOG(BER) VALUES FOR ALL USERS UNDER CA AND AT A TRANSMISSION DISTANCE OF 1500 M

Users	HG modes	Polarization state	Log(BER)
1	HG00	X-PL	-8
2	HG01		-7.77
3	HG10		-7.64
4	HG11		-7.63
5	HG00	Y-PL	-8.49
6	HG01		-7.82
7	HG10		-7.77
8	HG 11		-7.94

for other users (5–8) using same four HG modes transmitted on Y-PL. One can notice that as FSO range increments, the log(BER) also increments, while the users 1 and 5 that are using HG00 modes while propagating in FSO channel achieve the best performance when compared to other users that are using higher HG modes. Users 4 and 8 propagated using HG11, achieved a lower log (BER) than other users who propagated using lower order of HG modes. The log(BERs) of users 1, 4, 5, and 8 are -8, -7.6, -8.49, and -7.94, respectively, at the FSO link of 1400 m. As the acceptable value of log(BER) in FSO is approximately 6 [30], so all the information streams that were transmitted using different HG modes and two polarization states were successfully received at the transmission distance of 1500 m (100 m MMF + 1400 m FSO link), as all users had log(BER) less than -7. Additionally, the wider eye openings for all users at 1500 m (100 m MMF + 1400 FSO link) reveal reliable received data.

Table III shows the log(BER) values for the all users at a 1500 m (100 m MMF + 1400 FSO link) under CA weather conditions.

C. Effect of Weak and Strong Turbulence on the Performance of Proposed Model

The variations in temperature cause atmospheric turbulence, which degrades the performance of the information signal during its transfer in the FSOC channel. The turbulence varies from WT that has C_n^2 of 5×10^{-16} $\mathrm{m}^{\frac{-2}{3}}$ to ST that has C_n^2 of 5×10^{-14} $\mathrm{m}^{\frac{-2}{3}}$ [30], [48]. The effect of WT and ST on the performance of the proposed PDM/MDM based MMF/FSOC transmission in terms of log(BER) and different FSO is depicted in Fig. 8. A fixed MMF of 100 m is considered. It is clear that when the turbulence is strong, all the users that transmitted on either X-PL or Y-PL using four different HG modes (HG00, HG01, HG10, and HG11) achieved a propagation range of 1400 m with log(BER) approximately -4. On the other hand, the performance for the eight users using the proposed model becomes better when there is WT, as at the same FSO range of 1400 m, the log(BER) enhances and becomes ~ -6. As the acceptance limit for the log(BER) is < 6, so all the information data transmitted by the eight users (80 Gbps) is successfully received.

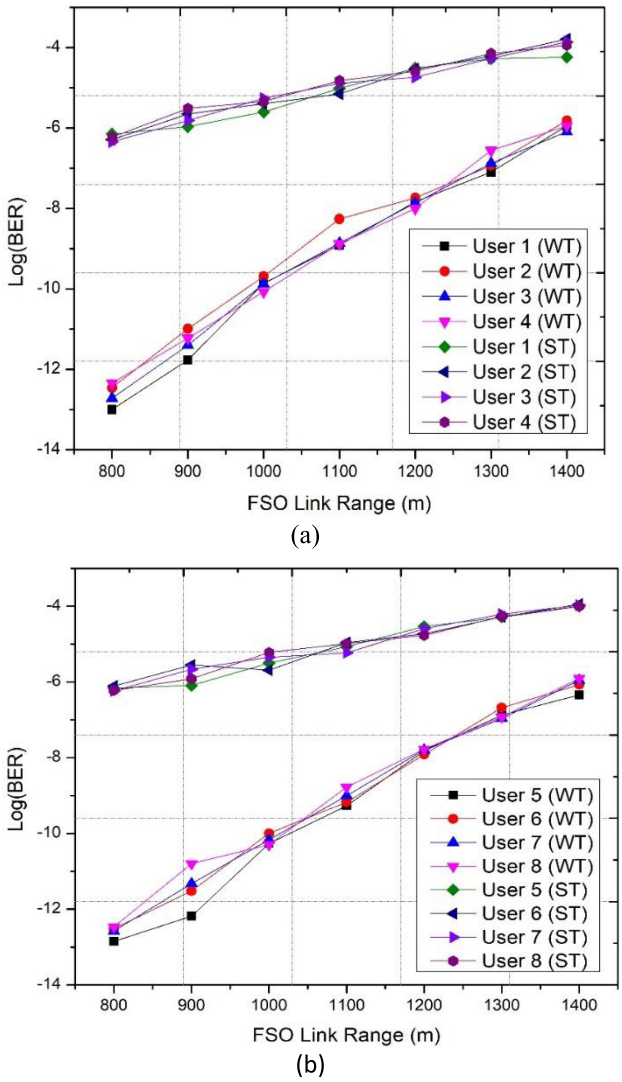

Fig. 8. Log(BER) for proposed PDM/MDM based MMF/FSOC transmission after a fixed MMF of 100 m versus different FSO links under WT and ST for (a) users 1–4 transmitted on X-PL and (b) users 5–8 transmitted on Y-PL.

Table IV summarizes the log(BER) values for all users under WT and ST at a distance of 1500 m (100 m MMF + 1400 FSO link).

D. Performance of Proposed Model for Varying MMF Cable Length

In this part, the effect of the MMF cable length on the performance of the proposed PDM/MDM based MMF/FSO transmission is discussed. A fixed FSO link of 100 m, ideal scintillation, and CA weather conditions are considered in this case. Fig. 9 presents the relation between the performance in terms of log(BER) of all users and the MMF length. For eight users, a shorter MMF length gives better performance than a longer MMF length. As an example, at an MMF length of 150 m, user 1 transmitted using HG00 mode and on X-PL has log(BER) $= -15.28$, while this value increases to -7.30 when the length of the MMF is prolonged to 250 m. Also, the eye diagram for

TABLE IV
LOG(BER) VALUES FOR ALL USERS UNDER WT AND ST AT A TRANSMISSION DISTANCE OF 1500 M

Users	HG modes	Polarization state	Log(BER)	
			WT	ST
1	HG00	X-PL	-5.95	-4.23
2	HG01		-5.81	-3.78
3	HG10		-6.09	-3.86
4	HG11		-5.94	-3.93
5	HG00	Y-PL	-6.34	-4
6	HG01		-6.09	-3.94
7	HG10		-5.94	-3.97
8	HG 11		-5.90	-4

TABLE V
LOG(BER) VALUES FOR ALL USERS CORRESPONDING TO 350 M (250 M MMF + 100 M FSOC LINK)

Users	HG modes	Polarization state	Log(BER)
1	HG00	X-PL	-7.30
2	HG01		-7.29
3	HG10		-7.28
4	HG11		-7.24
5	HG00	Y-PL	-7.27
6	HG01		-7.18
7	HG10		-7.27
8	HG 11		-7.23

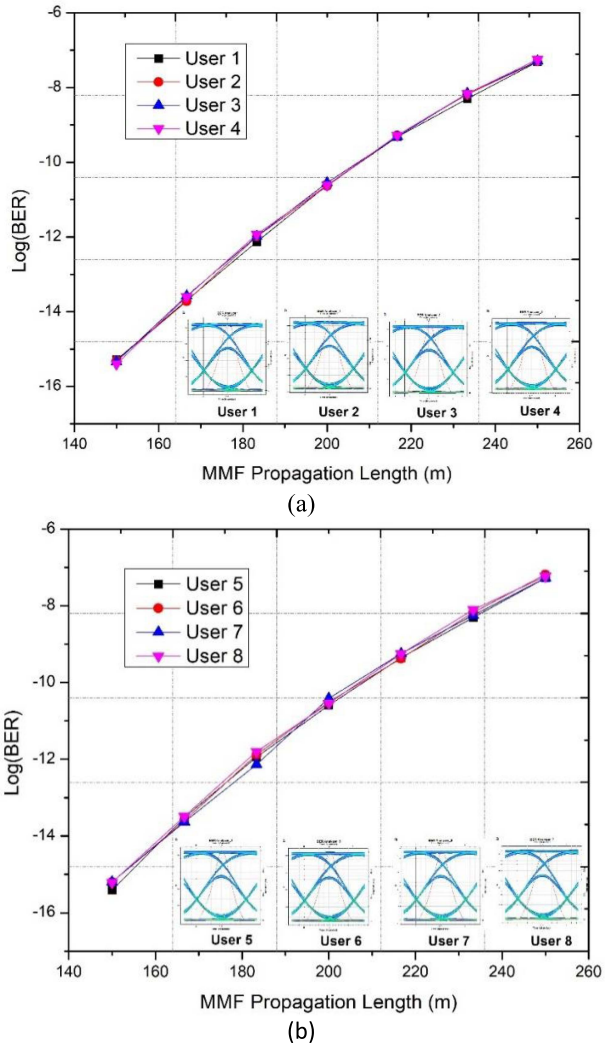

Fig. 9. Log(BER) for proposed PDM/MDM based MMF/FSOC transmission versus different MMF lengths for (a) users 1–4 transmitted on X-PL and (b) users 5–8 transmitted on Y-PL.

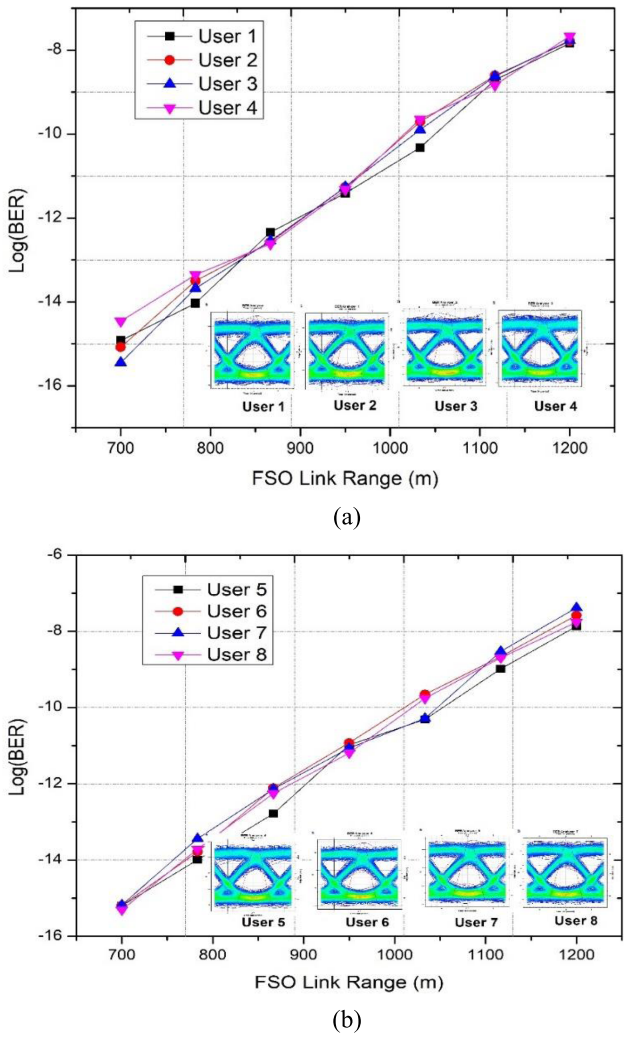

Fig. 10. Log(BER) for proposed PDM/MDM based MMF/FSOC transmission versus FSO range in Alexandria for (a) users 1–4 transmitted on X-PL and (b) users 5–8 transmitted on Y-PL.

the eight users at a 250 m MMF and a 100 m FSO reveal a successful transmission of 80 Gbps data. Additionally, one can notice that the performance of the proposed model is restricted as in the fiber there are nonlinearities present.

Table V shows the values of the log(BER) for the 8 users corresponding to 350 m (250 m MMF + 100 m FSOC range) under CA.

TABLE VI
COMPARISON BETWEEN PRESENT WORK AND PREVIOUSLY PUBLISHED WORKS

Ref.	Technique	Channel	Turbulence effect	Meteorological data	Overall capacity
[28]	PDM with OCDMA	FSO only	Not considered	Not considered	60 Gbps
[18]	OFDM with OCDMA	FSO only	Not considered	Not considered	45 Gbps
[51]	OOK	SMF + FSOC	Not considered	Not considered	10 Gbps
[52]	16-quadrature amplitude modulation	SMF + FSOC	Not considered	Not considered	10 Gbps
[53]	MDM	SMF + FSOC	Not considered	Not considered	40 Gbps
Present work	PDM with MDM	MMF + FSOC	WT and ST	Alexandria in Egypt, Pune in India, and Jeddah in KSA	80 Gbps

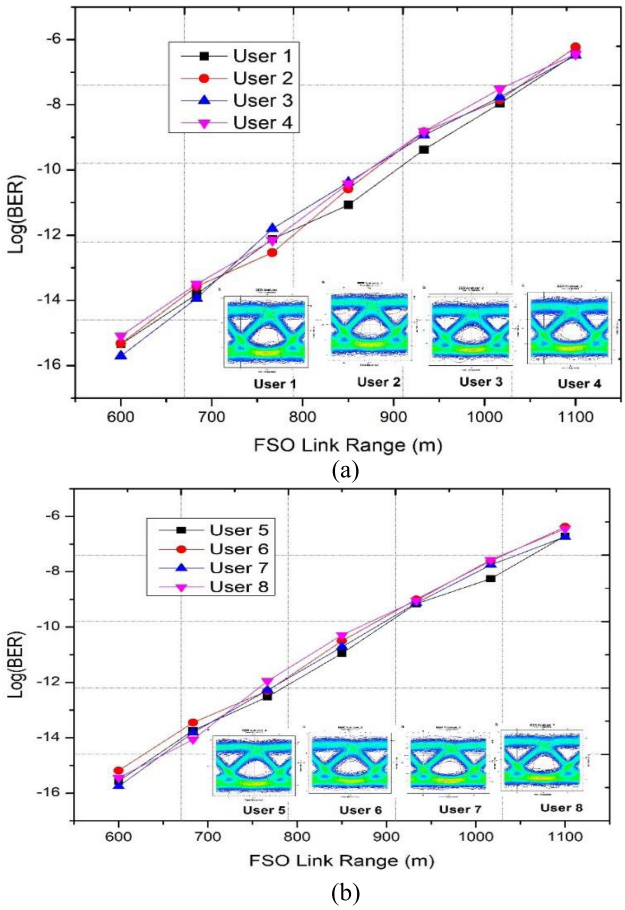

Fig. 11. Log(BER) for proposed PDM/MDM based MMF/FSOC transmission versus FSO range in Pune for (a) users 1–4 transmitted on X-PL and (b) users 5–8 transmitted on Y-PL.

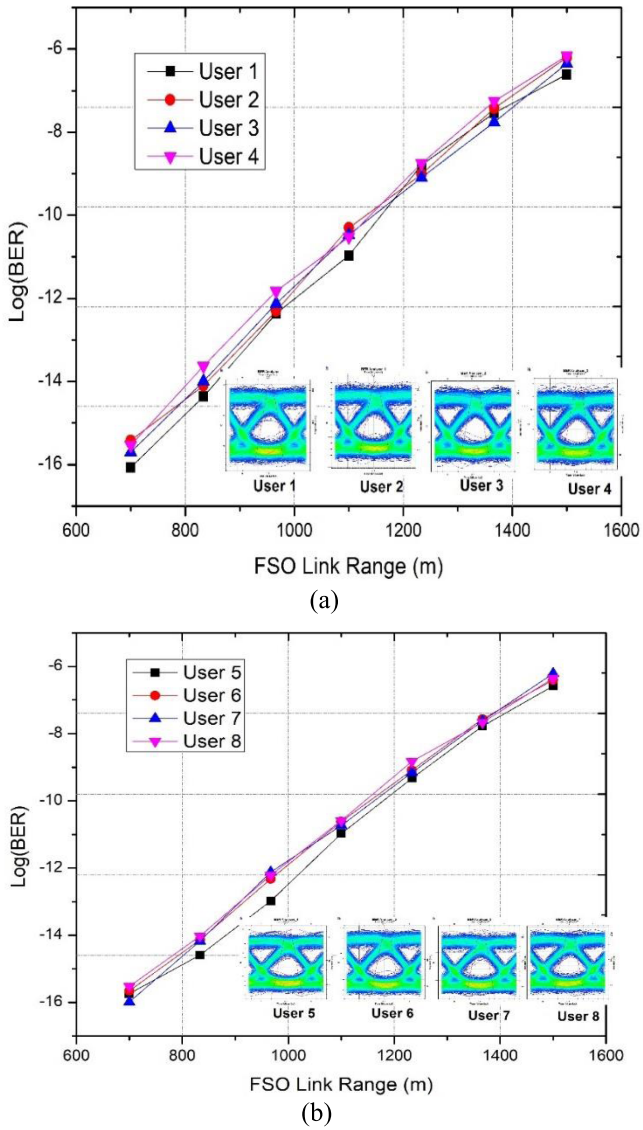

Fig. 12. Log(BER) for proposed PDM/MDM based MMF/FSOC transmission versus FSO range in Jeddah for (a) users 1–4 transmitted on X-PL and (b) users 5–8 transmitted on Y-PL.

E. Performance of Proposed Model for Cities Located in Three Different Countries

As to be able to show the availability of implement the proposed model in real environment, so the simulation parameters

are chosen based on real practical studies and the real meteorological data for different cities have various geographical data are considered. The average rainfall intensities from years 2014 to years 2018 for Alexandria city in Egypt, Pune city in India, and Jeddah city in KSA are 1.14 mm/hr, 3.33 mm/hr, and 0.28 mm/hr according to meteorological data taken from www.worldweatheronline.com 'accessed on January 2023' and refs. [1], [45], [50]. As the relation between attenuation coefficient of rain, β_r, in dB/km and rainfall intensity, R_f, is [50]:

$$\beta_r = 1.07 R_f^{0.67} \tag{15}$$

So by using this relation, the attenuations are 1.17 dB/km for Alexandria, 2.4 dB/km for Pune, and 0.45 dB/km for Jeddah. Figs. 10–12 depicts the log(BER) performance versus different FSO ranges after a fixed 100 m length of MMF cable for Alexandria, Pune, and Jeddah cities, respectively. As Jeddah has the lowest attenuation, so the eight users that propagated on different HG modes and two polarization signals of the proposed model achieves the longest range of 1500 m when implemented in it. This range is decreased to 1200 m and 1100 m when applied under the weather of Alexandria and Pune, respectively, and that is expected as Pune has the highest attenuation. All these ranges are below log(BER) $= -6$.

A comparison between recent published works and present work is shown in Table VI.

VII. Conclusion

In this article, a novel $2 \times 4 \times 10$ Gbps PDM/MDM based MMF/FSOC transmission system is proposed for high speed transmission capacity network. Two polarization states, X-PL and Y-PL, are considered. Each polarization signal carries four HG modes (HG00, HG01, HG10, and HG11). A 10 Gbps data is transmitted on each HG mode results in overall data transmission of 80 Gbps (as eight users are used). Hybrid channels, MMF cable and FSOC are used. The performance is investigated for two cases: in the first case, a fixed MMF cable length of 100 m and various FSO ranges in the absence and presence of WT and ST are considered. Different MMF cables lengths and fixed FSO link of 100 m are considered in the second case. Moreover, the performance is evaluated for the weathers of Alexandria, Pune, and Jeddah. The simulation obtained results show that, all users can transmit their data successfully for propagation ranges of 1500 m (100 m MMF cable + 1400 FSOC link) in the presence of WT with log(BER) less than -7 for the first case. In the second case, the existence of the nonlinearities in the MMF lead to performance restriction so, the overall transmission distance achieved by eight users is 350 m (250 m MMF cable + 100 m FSO link). Finally, the transmission ranges achieved by eight users are 1300 m for Alexandria (100 m MMF cable + 1200 m FSO link), 1200 m for Pune (100 m MMF cable + 1100 m FSO link), and 1600 m for Jeddah (100 m MMF cable + 1500 m FSO link). Subsequently, our suggested model is recommended to be used in high transmission hybrid wired/wireless networks and in next generation PON applications like smart homes, and smart health cares. It is imperative to conduct experimental demonstrations of our model to account for real-time losses and intermodal crosstalk, and we suggest integrating other multiplexing techniques with the suggested model, like OCDMA and OFDM, to enhance transmission capacity.

References

[1] S. A. A. El-Mottaleb, M. Singh, A. Chehri, H. Y. Ahmed, M. Zeghid, and A. N. Khan, "Capacity enhancement for free space optics, transmission system using orbital angular momentum optical code division multiple access in 5G and beyond networks," *Energies*, vol. 15, no. 19, 2022, Art. no. 7100.

[2] B. Kantarci and H. T. Mouftah, "Bandwidth distribution solutions for performance enhancement in long-reach passive optical networks," *IEEE Commun. Surv. Tut.*, vol. 14, no. 3, pp. 714–733, Third Quarter 2012.

[3] A. Sharma and J. Malhotra, "Simulative investigation of FMCW based optical photonic radar and its different configurations," *Opt. Quantum Electron.*, vol. 54, 2022, Art. no. 233.

[4] H. Singh and N. Mittal, "Performance analysis of free space optical communication system under rain weather conditions: A case study for inland and coastal locations of India," *Opt. Quantum Electron.*, vol. 53, pp. 1–21, 2021.

[5] J. Mirza, S. Ghafoor, and A. Hussain, "A full duplex ultrawideband over free-space optics architecture based on polarization multiplexing and wavelength reuse," *Microw. Opt. Technol. Lett.*, vol. 62, pp. 3999–4006, 2020.

[6] C. B. Naila, A. Bekkali, K. Kazaura, and M. Matsumoto, "BPSK intensity modulated free-space optical communications using aperture averaging," in *Proc. IEEE Int. Conf. Photon.*, 2010, pp. 1–5.

[7] A. Amphawan, S. Chaudhary, R. Din, and M. N. Omar, "5Gbps HG 0,1 and HG 0,3 optical mode division multiplexing for RoFSO," in *Proc. IEEE 11th Int. Colloq. Signal Process. Appl.*, 2015, pp. 145–149.

[8] Z. Zhou, H. Zhang, L. Chun, and A. Sharma, "Performance analysis of duobinary and CSRZ modulation based polarization interleaving for high-speed WDM-FSO transmission system," *J. Opt. Commun.*, vol. 43, no. 1, pp. 147–152, 2022.

[9] N. N. Cikan and M. Aksoy, "A review of self-seeded RSOA based on WDM PON," *Can. J. Elect. Comput. Eng.*, vol. 42, no. 1, pp. 2–9, Winter 2019.

[10] A. Ghazi, S. Aljunid, A. Noori, S. Z. S. Idrus, C. Rashidi, and A. Al-Dawoodi, "Design & investigation of 10×10 gbit/s MDM over hybrid FSO link under different weather conditions and fiber to the home," *Bull. Elect. Eng. Inform.*, vol. 8, pp. 121–126, 2019.

[11] E. Harstead, D. Van Veen, V. Houtsma, and P. Dom, "Technology roadmap for time-division multiplexed passive optical networks (TDM PONs)," *J. Lightw. Technol.*, vol. 37, no. 2, pp. 657–664, Jan. 2019.

[12] T. Dong and G. Shen, "Traffic grooming for IP over WDM optical satellite networks," in *Proc. IEEE 13th Int. Conf. Opt. Commun. Netw.*, 2014, pp. 1–6.

[13] J. Armstrong, "OFDM for optical communications," *J. Lightw. Technol.*, vol. 27, no. 3, pp. 189–204, Feb. 2009.

[14] N. Bai et al., "Mode-division multiplexed transmission with inline few-mode fiber amplifier," *Opt. Exp.*, vol. 20, pp. 2668–2680, 2012.

[15] R.-J. Essiambre, G. Kramer, P. J. Winzer, G. J. Foschini, and B. Goebel, "Capacity limits of optical fiber networks," *J. Lightw. Technol.*, vol. 28, no. 4, pp. 662–701, Feb. 2010.

[16] D. Qian et al., "101.7-Tb/s (370 × 294-Gb/s) PDM-128QAM-OFDM transmission over 3 × 55-km SSMF using pilot-based phase noise mitigation," in *Proc. Opt. Fiber Commun. Conf. Expo. Nat. Fiber Optic Engineers Conf.*, 2011, pp. 1–3.

[17] S. Chaudhary, A. Sharma, X. Tang, X. Wei, and P. Sood, "A cost effective 100 Gbps FSO system under the impact of fog by incorporating OCDMA-PDM scheme," *Wireless Pers. Commun.*, vol. 116, pp. 2159–2168, 2020.

[18] M. Singh, J. Kriz, M. M. Kamruzzaman, V. Dhasarathan, A. Sharma, and S. A. Abd El-Mottaleb, "Design of a high-speed-OFDM-SAC-OCDMA-based FSO system using EDW codes for supporting 5G data services and smart city applications," *Front. Phys.*, vol. 10, 2022, Art. no. 934848.

[19] K. H. Shakthi Murugan, A. Sharma, and J. Malhotra, "Performance analysis of 80 Gbps Ro-FSO system by incorporating hybrid WDM-MDM scheme," *Opt. Quantum Electron.*, vol. 52, 2020, Art. no. 505.

[20] A. Sharma and J. Malhotra, "Performance enhancement of photonic radar sensor for detecting multiple targets by incorporating mode division multiplexing," *Opt. Quantum Electron.*, vol. 54, 2022, Art. no. 410.

[21] K. K. Upadhyay, S. Srivastava, N. K. Shukla, and S. Chaudhary, "High-speed 120 Gbps AMI-WDM-PDM free space optical transmission system," *J. Opt. Commun.*, vol. 40, pp. 429–433, 2019.

[22] G. Li, N. Bai, N. Zhao, and C. Xia, "Space-division multiplexing: The next frontier in optical communication," *Adv. Opt. Photon.*, vol. 6, pp. 413–487, 2014.

[23] H. A. Fadhil et al., "Optimization of free space optics parameters: An optimum solution for bad weather conditions," *Optik*, vol. 124, pp. 3969–3973, 2013.

[24] M. Singh, A. Atieh, A. Grover, and O. Barukab, "Performance analysis of 40 Gb/s free space optics transmission based on orbital angular momentum multiplexed beams," *Alexandria Eng. J.*, vol. 61, no. 7, pp. 5203–5212, 2022.

[25] S. Chaudhary and A. Amphawan, "High-speed MDM-Ro-FSO system by incorporating spiral-phased Hermite Gaussian modes," *Photonic Netw. Commun.*, vol. 35, pp. 374–380, 2018.

[26] H. Kogelnik and T. Li, "Laser beams and resonators," *Appl. Opt.*, vol. 5, pp. 1550–1567, 1966.

[27] S. Chaudhary, S. Choudhary, X. Tang, and X. Wei, "Empirical evaluation of high-speed cost-effective Ro-FSO system by incorporating OCDMA-PDM scheme under the presence of fog," *J. Opt. Commun.*, vol. 39, pp. 1–4, 2020.

[28] S. A. Abd El-Mottaleb, A. Métwalli, T. A. ElDallal, M. Hassib, H. A. Fayed, and M. H. Aly, "Performance evaluation of PDM/SAC-OCDMA-FSO communication system using DPS code under fog, dust and rain," *Opt. Quantum Electron.*, vol. 54, 2022, Art. no. 750.

[29] C. Zhang et al., "Performance analysis of mode division multiplexing-based free space optical systems for healthcare infrastructure's," *Opt. Quantum Electron.*, vol. 53, pp. 635–648, 2021.

[30] M. Kumari, A. Sharma, and S. Chaudhary, "High-speed spiral-phase donut-modes-based hybrid FSO-MMF communication system by incorporating OCDMA scheme," *Photonics*, vol. 10, 2023, Art. no. 94.

[31] T. Kodama et al., "First. demonstration of a scalable MDM/CDM optical access system," *Opt. Exp.*, vol. 22, pp. 12060–12069, 2014.

[32] T. Kodama et al., "Asynchronous MDM-OCDM-based 10G-PON over 40km-SMF and 2km-TMF using mode MUX/DeMUX at remote node and OLT," in *Proc. Opt. Fiber Commun. Conf.*, 2014, Paper W2A.9.

[33] M. Born and E. Wolf, *Principles of Optics: Electromagnetic Theory of Propagation, Interference and Diffraction of Light*. Amsterdam, The Netherlands: Elsevier, 2013.

[34] M. Yan and L. Ma, "Generation of higher-order Hermite–Gaussian modes via cascaded phase-only spatial light modulators," *Mathematics*, vol. 10, 2022, Art. no. 1631.

[35] L. C. Andrews and R. L. Phillips, *Laser Beam Propagation Through Random Media*, 2nd ed. Bellingham, WA, USA: SPIE, 2005.

[36] H. Laabs, "Propagation of Hermite-Gaussian-beams beyond the paraxial approximation," *Opt. Commun.*, vol. 147, pp. 1–4, 1998.

[37] K. Kiasaleh, "Spatial beam tracking for Hermite-Gaussian-based free-space optical communications," *Opt. Eng.*, vol. 56, 2017, Art. no. 076106.

[38] X. Liu, D. Jiang, Y. Zhang, L. Kong, Q. Zeng, and K. Qin, "Propagation characteristics of Hermite-Gaussian beam under pointing error in free space," *Photonics*, vol. 9, 2022, Art. no. 478.

[39] A. E. Siegman, *Lasers*. Melville, NY, USA: University Science Books, 1986.

[40] S. Chaudhary et al., "40 Gbps-80 GHz PSK-MDM based Ro-FSO transmission system," *Opt. Quantum Electron.*, vol. 50, 2018, Art. no. 321.

[41] F. Mitschke, *Fiber Optics*. Berlin, Germany: Springer, 2016.

[42] A. W. Snyder and J. D. Love, *Optical Waveguide Theory*. London, U.K.: Chapman & Hall, 1983.

[43] R. Olshansky and S. M. Oaks, "Differential mode attenuation measurements ingraded-index fibers," *Appl. Opt*, vol. 17, no. 11, pp. 1830–1835, 1978.

[44] G. Xie et al., "Experimental demonstration of a 200-Gbit/s free-space optical link by multiplexing Laguerre-Gaussian beams with different radial indices," *Opt. Lett.*, vol. 41, pp. 3447–3450, 2016.

[45] H. Kaushal, V. Jain, and S. Kar, "Free-space optical channel models," in *Free Space Optical Communication. Optical Networks*. Berlin, Germany: Springer, 2017, pp. 41–89.

[46] D. A. Luong, T. C. Thang, and A. T. Pham, "Effect of avalanche photodiode and thermal noises on the performance of binary phase-shift keying-subcarrier-intensity modulation/free-space optical systems over turbulence channels," *IET Commun.*, vol. 7, pp. 738–744, 2013.

[47] J. Feng and X. Zhao, "Performance analysis of OOK-based FSO systems in Gamma-Gamma turbulence with imprecise channel models," *Opt. Commun.*, vol. 402, pp. 340–348, 2017.

[48] L. Li and A. Sharma, "High speed RGB-based duobinary-encoded visible light communication system under the impact of turbulences," *Front. Phys.*, vol. 10, 2022, Art. no. 944623.

[49] F. S. Vetelino, C. Young, L. Andrews, and J. Recolons, "Aperture averaging effects on the probability density of irradiance fluctuations in moderate-to-strong turbulence," *Appl. Opt.*, vol. 46, pp. 2099–2108, 2007.

[50] H. Singh, N. Mittal, and H. Singh, "Evaluating the performance of free space optical communication (FSOC) system under tropical weather conditions in India," *Int. J. Commun. Syst.*, vol. 35, no. 18, 2022, Art. no. e5347.

[51] C.-H. Yeh et al., "Hybrid free space optical communication system and passive optical network with high splitting ratio for broadcasting data traffic," *J. Opt.*, vol. 20, pp. 125702–125707, 2018.

[52] G. C. Mandal, R. Mukherjee, B. Das, and A. S. Patra, "Next-generation bidirectional triple-play services using RSOA based WDM radio on free-space optics PON," *Opt. Commun.*, vol. 411, pp. 138–142, 2018.

[53] H. Singh, N. Mittal, R. Miglani, and A. K. Majumdar, "Mode division multiplexing (MDM) based hybrid PON-FSO system for last-mile connectivity," in *Proc. IEEE 3rd South Amer. Colloq. Visible Light Commun.*, 2021, pp. 1–6.